



# Exposure-safety Markov modeling of ocular adverse events in patient populations treated with tisotumab vedotin

Summer Feng<sup>1,7</sup> · Rudy Gunawan<sup>2</sup> · Chaitali Passey<sup>1</sup> · Jenna Voellinger<sup>2</sup> · Daniel Polhamus<sup>3</sup> · Arnout Gerritsen<sup>4</sup> · Christine O'Day<sup>2</sup> · Anne-Sophie Carret<sup>2,5</sup> · Ibrahima Soumaoro<sup>1</sup> · Manish Gupta<sup>1</sup> · William D. Hanley<sup>2,6</sup>

Received: 4 November 2024 / Accepted: 26 August 2025  
© The Author(s) 2025

## Abstract

Tisotumab vedotin (TV), a tissue factor-directed antibody-drug conjugate (ADC), is approved in the US at 2.0 mg/kg every 3 weeks (Q3W) for adult patients with recurrent or metastatic cervical cancer following disease progression on or after chemotherapy. Previous logistic regression analysis showed a positive association between TV exposure and ocular adverse events (OAEs), which were identified as prespecified AEs of interest in TV clinical studies. To further optimize TV dose from a safety perspective, we developed a discrete-time Markov model (DTMM) to characterize exposure-response (E-R) relationships of exposures of both ADC and the microtubule-disrupting agent monomethyl auristatin E to the incidence, severity, and longitudinal time course of grade $\geq 2$  OAEs in patients with advanced solid tumors. A total of 757 patients who received TV as monotherapy or combination (with carboplatin, bevacizumab, or pembrolizumab) across seven clinical studies were included in this analysis. Of multiple covariates modeled, implementation of an eye care plan was the only covariate to significantly reduce risk of grade $\geq 2$  OAEs. The DTMM suggested an association between ADC exposure and risk of grade $\geq 2$  OAEs. Based on the totality of data from clinical outcomes, pharmacokinetics, and E-R analyses, as well as DTMM modeling results, TV 1.7 mg/kg every 2 weeks may provide higher efficacy with slightly increased risk of OAEs compared with 2.0 mg/kg Q3W, although these OAEs are manageable with an appropriate eye care plan. ClinicalTrials.gov ID (first submission): NCT03485209 (2018–03-08), NCT03657043 (2018–08-22), NCT03438396 (2018–02-08), NCT03786081 (2018–12-13), NCT03913741 (2019–03-29), NCT02001623 (2013–11-14), and NCT02552121 (2015–09-14).

**Keywords** Ocular adverse events · Markov model · Antibody-drug conjugate · Tisotumab vedotin · Oncology

## Introduction

Tisotumab vedotin (TV) is a tissue factor (TF)-directed antibody-drug conjugate (ADC) composed of a fully human monoclonal immunoglobulin-1 antibody specific for

TF, covalently linked to the microtubule disrupting agent monomethyl auristatin E (MMAE) via a protease-cleavable linker [1]. TV is directed to and internalized by cells expressing TF where it undergoes lysosomal degradation and release of the cytotoxic payload [1, 2]. Bystander killing can be induced by diffusion of free unconjugated MMAE over the cell membrane, leading to cytotoxicity against neighboring tumor cells [1, 3]. TV was the first TF-directed ADC approved by the US Food and Drug Administration for the treatment of adult patients with recurrent or metastatic cervical cancer with disease progression on or after chemotherapy [4].

The approved TV monotherapy dose of 2.0 mg/kg every 3 weeks (Q3W) demonstrated overall survival benefit with a manageable safety profile compared with chemotherapy in women with previously treated recurrent or metastatic cervical cancer [4, 5]. TV is also being investigated as

✉ Summer Feng  
sufe@genmab.com

<sup>1</sup> Genmab US, Inc., Plainsboro, NJ, USA

<sup>2</sup> Pfizer Inc., Bothell, WA, USA

<sup>3</sup> Metrum Research Group, Tariffville, CT, USA

<sup>4</sup> Genmab, Utrecht, the Netherlands

<sup>5</sup> Present address: Menarini Stemline, New York, NY, USA

<sup>6</sup> Present address: BeiGene, San Carlos, CA, USA

<sup>7</sup> 777 Scudders Mill Rd, Princeton, NJ 08536, USA

combination therapy and at alternative dosing regimens as monotherapy, for example, in the ongoing innovaTV 207 clinical trial in patients with non-cervical solid tumors [6]. Alternative dosing regimens, including those with more frequent administration, have the potential to optimize the range of pharmacokinetic (PK) exposures, resulting in improved clinical efficacy, provided safety and tolerability remain acceptable.

Ocular adverse events (OAEs) frequently occur in patients treated with a number of ADCs therapies across various tumor types [7, 8]. OAEs may occur due to on-target and off-target effects of ADCs. TV is directed to TF, which is a key component in initiating the coagulation cascade and has been shown to promote tumor growth, angiogenesis, and metastasis [9–12]. TF is expressed on cell membranes across a number of different organs, including the eyes, brain, and heart [13]. Expression of TF on the ocular epithelium could contribute to the development of OAEs, typically conjunctivitis, dry eye, blepharitis, and keratitis, which have been observed among patients treated with TV [5, 14].

Among 425 patients with recurrent or metastatic cervical cancer who received TV across clinical trials at the approved dosing regimen (2.0 mg/kg Q3W), OAEs were observed in 55% [4]. An eye care plan (ECP) was instituted during the phase I innovaTV 201 study, with the goal of minimizing the risk of OAEs with TV and was mandated in subsequent clinical studies [14]. The ECP includes prophylactic steroid and vasoconstrictor eye drops prior to each infusion, cold packs during infusion, lubricating eye drops throughout treatment and partnership with eye care professionals for prompt referral and management in case of OAEs. Dose modifications were mandated by study protocols as a management strategy for OAEs [5, 15].

The approved TV dosing regimen of 2.0 mg/kg Q3W for cervical cancer was supported by population PK and

exposure–response (E-R) analyses conducted using data across four clinical studies [16], and this dosing regimen also resulted in favorable antitumor activity in patients with previously treated head and neck squamous cell carcinoma (HNSCC) [17]. Additional modeling work using a population-PK-tumor growth inhibition (PPK-TGI) model suggested that higher dose intensity may improve efficacy [18]; specifically, 1.7 mg/kg every 2 weeks (Q2W) was selected for further investigation. This dosing regimen demonstrated encouraging antitumor activity and a manageable safety profile in line with prior TV monotherapy data in part C of the phase 2 innovaTV 207 (previously treated HNSCC) [19], albeit in a small cohort of patients. Adding to the limited clinical data, the current analysis aims to assess the risk of OAEs with more frequent TV dosing.

In the previous E-R analysis, the association between TV exposure and probability of occurrence of OAE was characterized using logistic regression analysis, but due to the limitation of the logit model, neither onset time nor duration of OAEs, critical factors in determining an alternate dosing regimen, were taken into consideration [18]. The current analysis develops an exposure–response model to describe the time course of grade  $\geq 2$  OAEs in patients with solid tumors treated with TV as monotherapy or in combination, and to evaluate the effects of TV exposure and covariate effects on risk of grade  $\geq 2$  OAEs. This model incorporated severity, onset, and duration of OAEs, as well as observed TV dosing history. Furthermore, to characterize OAEs under actual dosing conditions (e.g., considering dose delays or modifications and discontinuations due to AEs), a system of exposure-driven safety models was developed. From the models, predicted OAE profiles from alternative dosing regimens (Fig. 1), along with predicted dose modification behavior, could inform dose optimization in TV clinical studies.

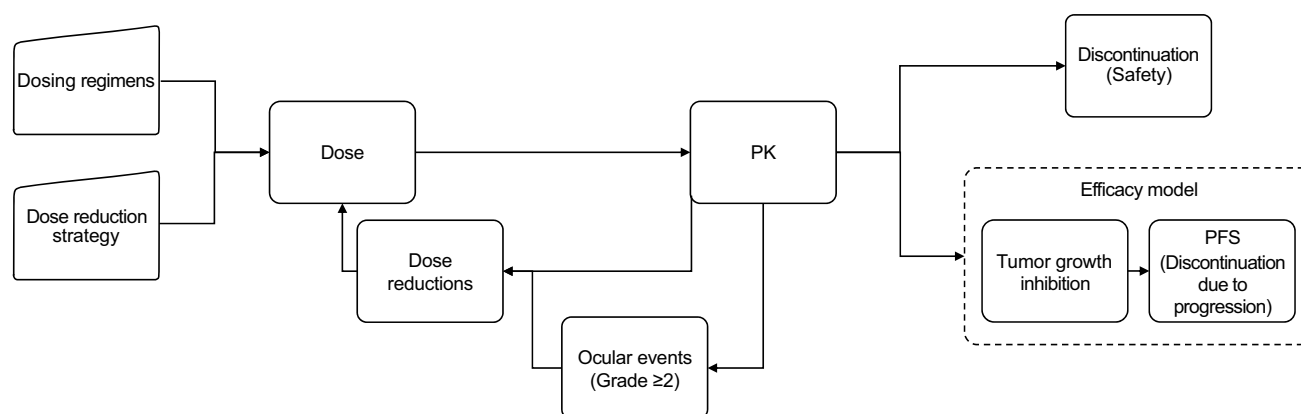


**Fig. 1** Simulation flowchart describing modeled endpoints and trial simulation routine. Trapezoidal shapes indicate inputs to the model and arrows indicate directionality of information and outputs. Dashed

rectangle refers to efficacy modeling (not reported here). PFS, progression-free survival; PK, pharmacokinetics

## Methods

### Patients and study design

This study was a retrospective analysis using pooled data from seven clinical studies of TV monotherapy and combination therapies in patients with advanced solid tumors: innovaTV 201 [14], innovaTV 202 [20], innovaTV 204 [5], innovaTV 205 [21], innovaTV 206 [22], innovaTV 207 [6], and innovaTV 208 [23].

All clinical studies were conducted in accordance with good clinical practice guidelines from the International Council for Harmonization of Technical Requirements for Pharmaceuticals for Human Use and the principles of the Declaration of Helsinki. Protocols were approved by relevant regulatory and independent ethics committees. Written informed consent was obtained from all patients enrolled in the clinical studies.

### Data analysis

Actual patient dosing records, including dose reductions, were included in the PK dataset. PK empirical Bayes estimates from the previously derived population-PK dataset were used to generate TV exposure metrics [24]. This model was translated to mrgsolve to facilitate simulation of several PK metrics, including longitudinal ADC, unconjugated MMAE payload concentrations, daily average concentration during the dosing interval, daily maximum concentration in the dosing interval, and area under the concentration–time curve at 6 weeks. These PK metrics were explored as exposure measurement in the subsequent E-R analyses.

The OAE dataset included AE severity grades 0, 1, 2, and  $\geq 3$  based on the day of occurrence and duration of OAEs. Across trials, AEs, including OAEs, were assessed and reported at each study visit; visit schedules for each study are shown in Supplementary Table 1. OAEs were graded according to both ophthalmological grading (assessed by the ophthalmologist during ophthalmological evaluation) and CTCAE grading system (assessed by the investigator based on NCI-CTCAE criteria). OAEs were graded according to CTCAE version 4.3 in the innovaTV 201 and innovaTV 202 trials, and according to CTCAE version 5.0 in the innovaTV 204, innovaTV 205, innovaTV 206, innovaTV 207 and innovaTV 208 trials. OAEs were regarded as AEs of special interest across all 7 clinical trials.

To support the characterization of OAEs, both a three-state Markov model (grade  $\leq 1$ , grade 2, and grade  $\geq 3$ ) and a simplified two-state model (grade  $\leq 1$  vs grade  $\geq 2$ ) were developed. The three-state model enables more granular evaluation of OAE occurrence across clinically relevant severity levels, while the two-state model offers a

streamlined framework to evaluate the overall burden of moderate-to-severe ocular toxicity. To allow for estimation of a Markovian element, the status for a patient's previous day was also incorporated. OAE data used to generate the exposure-OAE model included TV as monotherapy and TV in combination with other treatments across several tumor types (tumors of the ovary, cervix, endometrium, bladder, prostate, or esophagus, head and neck squamous cell carcinoma, non-small cell lung cancer, colorectal cancer, or exocrine pancreatic cancer) from the above-mentioned trials.

The effect of covariates on the risk of grade  $\geq 2$  OAEs was also evaluated. These covariates included TV therapy type (as monotherapy or in combination with pembrolizumab, carboplatin, or bevacizumab), TV dose and schedule, presence of OAEs at baseline that were not specified as exclusion criteria, presence of dry eyes at baseline, and whether ECP was mandated (15 patients from innovaTV 201 were enrolled prior to implementation of the ECP). Each study protocol specified ongoing or cicatricial ocular surface conditions at the time of enrollment as exclusion criteria; however abnormal ocular baseline findings alone were generally not a reason for exclusion from the studies [5, 6, 20–23]. OAE durations were imputed in cases where the OAE start (missing in  $<1\%$  of cases) or end date (missing in  $\approx 20$ – $30\%$  of cases) was missing. Missing end dates were more prevalent in the less serious grade 1 events (25%) and less prevalent for grade  $\geq 2$  events ( $\sim 10\%$ ), and the missingness pattern was consistent across treatment regimens. For these missing records, OAE duration was set to within-study median OAE durations. Apart from OAE durations, no other imputation of analysis variables was performed.

The dosing regimen and timing of dose modifications, often resulting from AEs, directly affect exposure. Therefore, data on dose reductions and treatment-related AEs (TRAEs) leading to discontinuation were also included to facilitate competing risk/time-to-event model development for the integrated simulation of OAEs. The day of discontinuation due to TRAEs was censored by discontinuation for other reasons (e.g., disease progression, investigator decision). To account for varying treatment durations and observation windows across subpopulations of patients, discontinuation due to progression was also captured for modeling, with times for patients discontinuing due to reasons other than progression (e.g., TRAEs, investigator decision) being censored.

### Summary of data source

Observed OAEs were tabulated and summarized graphically across regimens and studies. In addition, the time profile and prevalence of the grades of OAE were illustrated using stacked area plots, stacked frequency plots, and percentage

of patients by grade of event, time, study, and regimen (Supplementary Table 1 and Supplementary Fig. 2).

## Model development

The relationships between exposure and the incidence, severity, and time course of daily grade  $\geq 2$  OAEs were characterized using a discrete time Markov model (DTMM) with a first-order Markov element on daily intervals, logit link relating predictors to cumulative state probabilities, and interindividual variability (IIV) on baseline probabilities [25, 26]. The impact of ADC and MMAE exposure, as well as other covariates (e.g., coadministration of pembrolizumab and baseline dry eye), on transition probabilities between grade  $\leq 1$  and  $\geq 2$  OAEs were evaluated. Model diagnostics were used to select covariates that were associated with residual trend or model misspecification from a prespecified list. Covariates were added in a single forward step, resulting in a modified “full model” approach [27]. As shown in Fig. 2, various combinations of the exposure models (e.g., direct and effect compartment), transformations (e.g., linear and hyperbolic), and functional inclusions of IIV (i.e., on transition probabilities, half maximal effective concentration, and the rate constant for the effect compartment) were also assessed during model development.

A base OAE model was first developed that included only structural parameters and exposure. Covariates were added to this model as guided by model evaluation to arrive at a final model. The occurrence (and duration) of OAE events was modeled with either two or three categories: OAE occurrence of grade  $\geq 2$ , or of grade 2 and grade 3 separately. The DTMM was specified by including a Markov

component using a proportional-odds model structure, as shown in formula below for patient  $i$  on day  $j$ :

$$\begin{aligned} & \text{logit} [P(OAE_{i,j} \geq m | OAE_{\{i,j-1\}} = k)] \\ &= \log \left( \frac{P(OAE_{i,j} \geq m | OAE_{\{i,j-1\}} = k)}{1 - P(OAE_{i,j} \geq m | OAE_{\{i,j-1\}} = k)} \right) \\ &= \beta_{mk}^0 + D(t_{ij}, f(C_{ij}^{ADC}, \beta^{ADC}), g(C_{ij}^{TOX}, \beta^{TOX})) \times \prod_{p=1}^P \gamma_p^{X_{ip}} \end{aligned}$$

where  $\beta_{mk}^0$  is the intercept for the logit probability of being at least in the current state ( $m$ ) of OAE given previous state of OAE  $k$ , where, in the case of three states,  $m \in [1-3]$  and  $k \in [1-3]$ . ADC represents parameters and concentrations of the ADC while TOX represents MMAE. The functional inclusion of exposure (both ADC and TOX) is represented as  $f()$  and  $g()$ , which are combined through function  $D()$ . This effect is then scaled by covariate effects  $\gamma$  across patient covariates  $x$ . As a result of the logit link, when  $D()$  is linear in the logit transform of the cumulative probabilities, the effects (e.g.,  $\beta^{ADC}$ ) are on the log odds of being at or above state  $m$  and are proportional across states. Allowing  $\beta^{ADC}$  and  $\beta^{TOX}$  to vary across states relaxes the proportionality assumption and results in non-proportionality adjustments (i.e., the “partial cumulative probability model”) [28].

Exposure functional forms are considered combinations of linear and hyperbolic functions of exposure. For example, a linear and additive adjustment of the direct ADC and TOX exposure effects on the log odds took the form:

$$\begin{aligned} & D(f(C^{ADC}(t), \beta^{ADC}(t)), g(C^{TOX}(t), \beta^{TOX}(t))) \\ &= \beta_1^{ADC} C^{ADC}(t) + \beta_1^{TOX} C^{TOX}(t) \end{aligned}$$

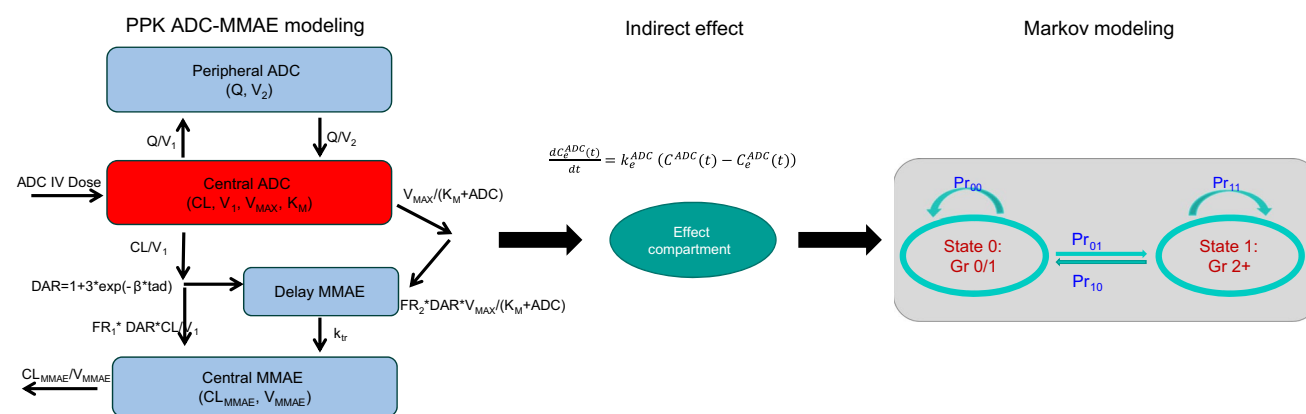


**Fig. 2** Final population PK and Markov model. Two-compartment ADC model with parallel linear and Michaelis–Menten elimination, a delay compartment, and a one-compartment unconjugated MMAE model 19. ADC, antibody–drug conjugate; CL, clearance; DAR, drug-to-antibody ratio; FR1, fraction of nonspecific elimination directed to the central compartment; FR2, fraction directed to the delay compartment;  $k_{tr}$ , delay compartment rate constant;  $E_{max}$ , maximum effect;

KM, Michaelis constant; MMAE, monomethyl auristatin E; PK, pharmacokinetics; Q, intercompartmental clearance;  $V_c$ , central volume of distribution;  $V_{max}$ , maximum Michaelis–Menten elimination rate;  $V_{MMAE}$ , apparent MMAE central volume of distribution;  $V_p$ , peripheral volume of distribution; Pr, probability;  $k_e^{ADC}$ , ADC effect compartment rate constant

Other functional forms included combinations of linear and hyperbolic/sigmoidal effects, e.g., hyperbolic in ADC and linear in TOX:

$$D(f(C^{ADC}(t), \beta^{ADC}(t)), g(C^{TOX}(t), \beta^{TOX}(t))) \\ = \frac{\beta_1^{ADC} C^{ADC}(t)}{\beta_2^{ADC} + C^{ADC}(t)} + \beta_1^{TOX} C^{TOX}(t)$$

Exposure itself, for either ADC or TOX, was represented as average concentration in the day ( $C$ ) or, in cases where a time delay between ADC or TOX PK and OAE was present, as  $C_e$  (denoting use of an effect compartment, or turnover model). When using an effect compartment (turnover model), the default representation was a first-order differential equation:

$$\frac{dC_e^{ADC}(t)}{dt} = k_e^{ADC} (C^{ADC}(t) - C_e^{ADC}(t)), \text{ where } k_e$$

is the ADC effect compartment rate constant. Transit compartment modeling was also considered in cases where time delays beyond the simple turnover model were indicated [29]. IIV was considered on the transition probabilities as well as drug effect parameters, on the logit and lognormal scales, respectively. When modeled, IIV was included as distributed according to a lognormal distribution. For example, when modeling IIV on transition probabilities:  $\beta_{mki}^0 = \beta_{mk}^0 e^{\eta_i}$ , where  $\eta_i \sim N(0, \omega^2)$ .

In addition to the characterization of the exposure–response relationships of OAEs, we characterized the relationship between exposure and dose reduction using a repeated time-to-event model, and the relationship between exposure and discontinuation (due to AE or disease progression) using a time-to-event model. For each of these, the hazard of event was modeled in a similar manner to that described for OAE modeling:

$$h(t_i) = h_0(t_i) \times D(f(C(t_i)^{ADC}, \beta^{ADC}), g(C(t_i)^{TOX}, \beta^{TOX})) \times \prod_{p=1}^P \gamma_p^{X_{ip}},$$

where  $h_0$  is the baseline hazard of discontinuation or dose reduction, modulated by exposure through  $D()$  and covariate effects  $\gamma$ . Choice of  $h_0$  induces a distributional form of the survival times and several parametric survival models were considered (Weibull, exponential, etc.). To ease the use of longitudinal ADC and TOX exposures, numerical integration of the hazard was used for all models in calculation of the likelihood; e.g.,  $L(t_i) = h(t_i)^{\delta_i} \times \exp\{-H(t_i)\}$ , where  $\delta_i$  indicates occurrence of an event (versus censoring) and  $H(t_i) = \int_0^{t_i} h(u) du$ .

In addition to these modeled endpoints, simulations from a previously published joint tumor growth index–OS model [18] were used to inform time to disease progression.

## Model selection criteria and evaluation

Model selection was guided by model convergence, convergence of the covariance step in NONMEM (Icon plc, Dublin, Ireland), precision, identifiability of parameter estimates, and Akaike information criterion (AIC).

Model evaluation relied primarily upon visual predictive checks (VPCs) in which the model was used to simulate observations that were conditional on observed covariates, dosing, fitted parameters, and observed censoring times. Statistics of the observed data were then compared with summaries of those statistics applied to simulations from the model. For the OAE model, model-predicted and observed time profiles of OAEs and transition probabilities were compared in order to evaluate the DTMM model. The first occurrence of grade  $\geq 2$  OAEs was also compared using Kaplan–Meier–type VPCs. The time to first and second dose reduction and discontinuation due to AEs were also compared between model-predicted and observed data in time-to-event models.

## Model application

To support further development of TV in non-cervical tumors, the time profile of OAEs was simulated at various dosing regimens accounting for dose reductions, discontinuation due to AE, and disease progression. The simulated OAE profiles of the more-frequent dosing regimen were compared with the profile at the approved dosing regimen of 2 mg/kg Q3W. The OAE, dose reduction, discontinuation, and projected disease progression were combined for joint exposure-driven simulations. When dose reduction events were simulated to have occurred, doses were reduced according to the following approximation of the protocol-specified dose reduction procedure for ocular event mitigation: only two total dose reductions could be experienced by a simulated patient (they discontinued treatment on the third), wherein each dose reduction decreased the dose relative to the last dose received by 30%. In addition, any simulated patient experiencing at least 6 consecutive weeks of grade  $\geq 2$  events discontinued at the sixth week of continuing events.

## Computational software

Data manipulation, visualization, and simulations were conducted using R version 4.1.1 (R Foundation, Vienna, Austria), a data-analysis language suitable for use in regulated environments (Institute for Statistics and Mathematics 2018). Analyses were conducted via NONMEM version 7.5. For simulations, mrgsolve was used to combine all individual models and incorporate the dynamic dose reduction



procedure [30]. All code was maintained using the version control system Subversion (Apache Software Foundation, Forest Hill, MD, USA). All analyses were conducted on a computer grid with multiple compute nodes. Each node ran the Ubuntu operating system (Ubuntu 18.04.5 LTS, Linux kernel 5.4.0–1054-aws) and used the GFortran compiler (version 7.5.0 for Linux; GNU Project, Boston, MA, USA).

## Results

### Patients and grade $\geq 2$ OAE frequencies

Details on the 757 patients in the analysis population are included in Supplementary Table 1. Most commonly, patients had received TV monotherapy 2.0 mg/kg Q3W ( $n=381$  [50%]), TV monotherapy 0.9 mg/kg on days 1, 8, and 15 of a 28-day cycle (3Q4W) ( $n=165$  [22%]), TV 2.0 mg/kg combined with pembrolizumab ( $n=74$  [10%]), or TV 2.0 mg/kg combined with carboplatin ( $n=40$  [5%]); the TV 2.0 mg/kg regimen was also combined with bevacizumab ( $n=9$  [1.2%]). For patients treated with TV monotherapy 2.0 mg/kg Q3W, which is the dosing regimen approved for patients with previously treated cervical cancer, the rate of grade  $\geq 2$  OAEs varied between 31% (phase 1 first-in-human innovaTV 201) and 7% (phase 2 innovaTV 204 that led to the accelerated approval of TV in the US). When TV was combined with either pembrolizumab, carboplatin, or bevacizumab, the grade  $\geq 2$  OAEs were observed in 32%, 32%, and 89% of patients, respectively (see Supplementary Table 1 for incidence by individual clinical trials). Across all seven studies, the probability of experiencing grade  $\geq 2$  OAEs peaked at around 8 weeks after first dose (Supplementary Fig. 2). Studies of TV monotherapy that included patients who were enrolled prior to implementation of ECP (innovaTV 201 and innovaTV 202) resulted in a numerically higher incidence of grade  $\geq 2$  OAEs (Supplementary Fig. 2).

### OAE model development

Base model structure was initially considered as a three-state OAE model (grade  $\leq 1$ , 2, and 3 OAE events). However, quantification of standard errors of parameter estimates

(i.e., convergence of the covariance step) was generally problematic due to low grade 3 OAE rates (models 1 to 5); as a result, the model was simplified to a two-state model (grades  $\leq 1$  and  $\geq 2$ ; Supplementary Table 3: model 1000). Using the two-state model, effects of longitudinal ADC and MMAE as linear or hyperbolic (e.g., maximum effect [ $E_{\max}$ ]) effects on the log-odds of event were compared (models 1000 to 1005), and then compared with the same functional forms acting on total ADC through an effect compartment ( $ADC_e$ ) and MMAE through an effect compartment ( $TOX_e$ ) (models 1100 to 1103). Generally, the use of an effect compartment gave improvements in model fit per AIC (e.g., model 1100 versus 1000; model 1102 vs 1002), and the  $E_{\max}$  functional forms of ADC and MMAE gave the lowest AIC (model 1102 vs 1100, and 1103). Throughout all joint models (i.e., including both ADC and MMAE), estimated exposure effects differed in direction, with ADC and  $ADC_e$  associated with increased odds of event and MMAE and  $TOX_e$  associated with lowering odds of event. In the absence of a mechanistic explanation for MMAE reducing the probability of OAEs, this result was interpreted as indicative that due to lack of identifiability, the direct E-R effects of unconjugated MMAE and ADC might not be separately estimable. Given the potential parameter-identifiability issues in model 2, as well as the need to further investigate the counterintuitive effect of unconjugated MMAE on risk of AEs, ADC alone was chosen as the exposure metric in the base model (Table 1: model 1102\_1).

Model development proceeded with the addition of covariate effects and testing of IIV on the exposure-dependent log odds of event through  $E_{\max}$  (Supplementary Table 3: model 40071). Model evaluation indicated presence of non-proportionality of the exposure effect between states, so an adjustment factor for the exposure effect when in the  $\geq 2$  state version was added (Table 1: model 40073). In the final model (model 40073) representation of exposure was a hyperbolic transformation of  $ADC_e$ , which included covariate adjustments for bevacizumab, carboplatin, pembrolizumab, presence of OAEs at baseline, presence of dry eyes at baseline, prophylactic treatment in patients enrolled prior to introduction of the ECP, and a non-proportionality adjustment to the exposure effect, with IIV included on the reference transition probabilities. The parameter estimates from final OAE model are presented in Table 2.

**Table 1** AIC and objective model function

	Model number	Description	Objective function	AIC
AIC Akaike information criterion, $ADC$ antibody–drug conjugate, $E_{\max}$ maximum effect, $IIV$ interindividual variability, $MMAE$ monomethyl auristatin E	1102_1	Base model: two-state; effect compartment, $E_{\max}$ ADC only; IIV on baseline	5638.663	5650.663
	1102_3	Two-state: effect compartment, $E_{\max}$ ADC only, linear function for unconjugated MMAE; IIV on baseline	5594.443	5608.443
	40073	Final model: $E_{\max}$ effect compartment of ADC, differing conditional effect across states; IIV on baseline; covariate model	5499.285	5525.285

**Table 2** Final model parameter estimates for OAEs (fixed effects)

			Estimate	95% CI
Structural model parameters				
$\beta_{01}^0$	$\exp(\theta_1)/(1 + \exp(\theta_1))$	Probability of transition to grade $\geq 2$ event from grade $\leq 1$	0.000209	0.000107–0.000408
$\beta_{11}^0$	$\exp(\theta_2)/(1 + \exp(\theta_2))$	Probability of staying in state 2+ from grade $\geq 2$	0.963	0.950–0.972
$\beta_1^{ADC}$	$\theta_3$	$E_{\max}$ for $ADC_e$	11.7	5.45–17.9
$k_{e,TV}^{ADC}$	$\exp(\theta_5)$	$ADC_e$ effect compartment rate constant	0.0389	0.0313–0.0484
$\zeta_{11}$	$\theta_6$	Nonproportionality adjustment for $ADC_e$ in event state	0.215	0.112–0.318
$\beta_3^{ADC}$	$\theta_7$	Hill parameter for $ADC_e$	1.00	FIXED
$\beta_2^{ADC}$	$\theta_{18}$	EC50 for $ADC_e$	4.91	0.158–9.66
Covariate effect parameters				
$\gamma_1$	$\theta_9$	$ADC_e$ -modifying effect of bevacizumab	1.25	0.901–1.59
$\gamma_2$	$\theta_{11}$	$ADC_e$ -modifying effect of carboplatin	0.920	0.710–1.13
$\gamma_3$	$\theta_{12}$	$ADC_e$ -modifying effect of pembrolizumab	1.07	0.887–1.25
$\gamma_4$	$\theta_{13}$	$ADC_e$ -modifying effect of baseline ocular conditions	0.887	0.518–1.26
$\gamma_5$	$\theta_{14}$	$ADC_e$ -modifying effect of dry eyes at baseline	1.36	0.747–1.97
$\gamma_6$	$\theta_{20}$	$ADC_e$ -modifying effect of ECP	0.685	0.581–0.789

Final model:

$$\text{logit}[P(OAE_{i,j} \geq 2 | OAE_{i,j-1} \leq 1)] = \beta_{01}^0 + \frac{\beta_1^{ADC} ADC_{e,i,j}}{\beta_2^{ADC} + ADC_{e,i,j}} \times \prod_{P=1}^P \gamma_P^{X_{i,P}} \times e^{\eta_i}$$

and

$$\text{logit}[P(OAE_{i,j} \geq 2 | OAE_{i,j-1} \geq 2)] = \beta_{m11}^0 + \frac{\beta_1^{ADC} ADC_{e,i,j}}{\beta_2^{ADC} + ADC_{e,i,j}} \times \prod_{P=1}^P \gamma_P^{X_{i,P}} \times e^{\eta_i} \times \zeta_{11}$$

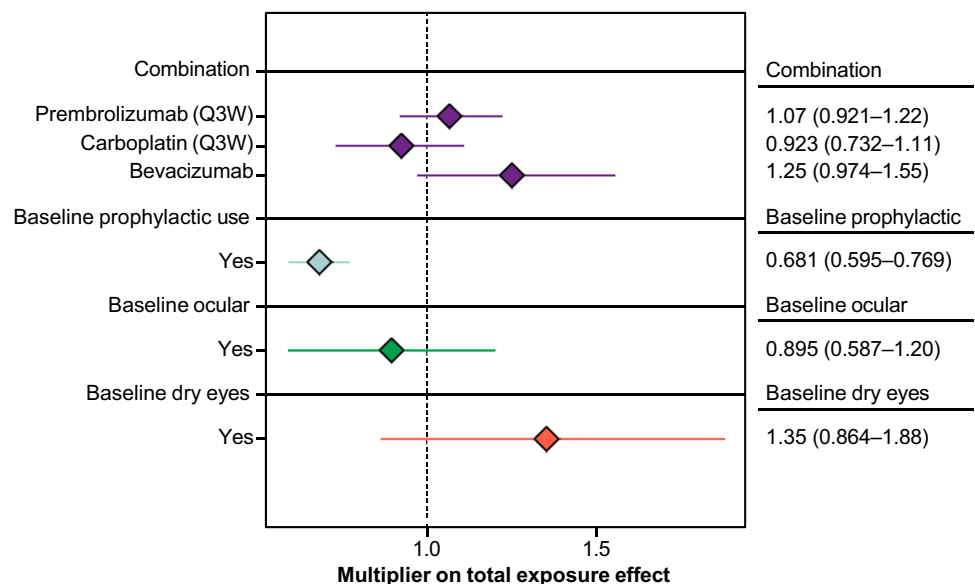
Parameters estimated in the log-domain were back-transformed for clarity. CIs = estimate  $\pm$  1.96  $\cdot$  SE

$ADC$  antibody–drug conjugate,  $ADC_e$  antibody–drug conjugate through an effect compartment; EC50, half maximal effective concentration; ECP, eye care plan;  $E_{\max}$ , maximum effect; OAE, ocular adverse event; SE, standard error

The exposure effects for 0.9 mg/kg 3Q4W, 1.2 mg/kg 3Q4W, and 2.0 mg/kg Q3W monotherapy indicated a dose-dependent, delayed-onset effect of exposure on the probability of grade  $\geq 2$  event occurrence. The exposure effects are included in Supplementary Fig. 4. Trough effect on the probability of grade  $\geq 2$  event occurrence was similar

between the 0.9 mg/kg 3Q4W and 2.0 mg/kg Q3W regimens, both of which were associated with a lower effect than the 1.2 mg/kg 3Q4W regimen. Covariate effects as multiplicative factors of the exposure effect indicated a decrease of 31.3% (90% confidence interval [CI]: 22.8–39.7) in patients enrolled in studies after the introduction

**Fig. 3** Covariate effect. Mean and 90% CI of indicated effect as a proportional effect (relative to the reference patient) on the total exposure effect on the log-odds of transition. The reference patient, who was treated with TV monotherapy, was studied prior to the ECP and had no baseline ocular events or baseline dry eye events. ECP, eye care plan; Q3W, every 3 weeks; TV, tisotumab vedotin



of the ECP. In all 3 models, there was a negligible influence detected for an increased risk of OAEs with TV+pembrolizumab (mean: 1.07, 90% CI: 0.921–1.22) or TV+carboplatin (mean: 0.923, 90% CI: 0.732–1.11) in comparison to TV monotherapy (Fig. 3). Numerical increases in the risk of OAEs were seen with TV+bevacizumab (mean: 1.25, 90% CI: 0.974–1.55) versus TV monotherapy and with the occurrence of dry eyes at baseline (mean, 1.35; 90% CI, 0.864–1.88); however, these trends were not statistically significant. Implementation of the ECP was the only factor associated with a reduced risk of OAEs (mean, 0.681; 90% CI, 0.595–0.769).

### Time-to-event model development

The time-to-dose-reduction model was an exponential survival model in which the ADC exposure entered linearly after passing through two transit compartments accounting for the delay–exposure effect. A decreased hazard after the first dose reduction was identified, as was decreased hazard in ovarian cancers relative to cervical cancers and in patients studied after introduction of the ECP. A decrease in hazard for patients with Eastern Cooperative Oncology Group status > 0 was also identified. Parameter estimates are included in Supplementary Table 5.

The Kaplan–Meier plot for observed data of discontinuation due to AE showed that patients treated with TV monotherapy appeared to have a more rapid time course of discontinuation due to AE, compared with those who received combination therapies (Supplementary Fig. 6). Time to discontinuation due to AE was an exponential survival model in which hazard was linearly dependent on exposure of ADC from the effect compartments. The effect of combination therapies, ECP, and tumor location were included in the final model based on AIC criteria, in which the model that included combination therapies, and ECP had much lower AIC relative to that in base model (AIC: 1730 vs 1765), with AIC dropping further when tumor location was included (AIC: 1724). Parameter estimates are included in Supplementary Table 7.

### Model evaluation

VPCs were used as the primary model-evaluation tool. Model evaluation plots by covariate are shown in Supplementary Fig. 8. Simulations of transition counts (to and from the event state) by primary regimens of interest demonstrated suitable replication of the observed data (Fig. 4a). The final Markov model provided a reasonable description of observed grade  $\geq 2$  OAE data by regimen (Fig. 4b). Plots for time-to-event of first occurrence of grade  $\geq 2$  OAE showed slight overprediction for patients who received 2.0 mg/kg

TV Q3W as monotherapy and experienced a grade  $\geq 2$  event at any point (Fig. 5). However, the time-to-first-incidence course for the combination therapies and other monotherapy regimens was captured sufficiently in the plots. Most first occurrences of grade  $\geq 2$  OAEs took place by approximately 14–21 weeks after therapy initiation. The time course of grade  $\geq 2$  OAEs was similar between monotherapy and combination therapies.

### Model application

Regimens of interest for non-cervical tumors were simulated using the final dose reduction, discontinuations due to AE, progression, and OAE models. At 13 weeks, approximately 13% of patients in all regimens were predicted to be experiencing grade  $\geq 2$  OAEs. After 13 weeks, a higher probability of dose reductions in the combination therapies resulted in a lowering of the OAE rate in those patients remaining on treatment (Supplementary Tables 9 and 10). Simulated dose reductions in monotherapy were less common, resulting in higher exposure and consequently higher probability of OAEs later in the time course, as well as higher probability of discontinuation due to AEs (Fig. 6). Higher dose intensities appeared to be associated with a higher risk of grade  $\geq 2$  OAEs in noncervical tumors (Fig. 6). The 2.0 mg/kg Q3W and 1.5 mg/kg Q2W regimens (see Supplementary Fig. 11 for simulated PK data) were associated with the lowest probability of OAE and were essentially equivalent, which could be the result of comparable PK profiles between these two dosing regimens.

### Discussion

Dose optimization is a continuously evolving effort and plays a critical role in drug development [31]. Dose optimization is particularly important with ADCs because they typically have a narrow therapeutic window relative to monoclonal antibodies used in cancer treatment [32]. Although the Q3W dosage regimen of TV has demonstrated effectiveness in recurrent or metastatic cervical cancer, ongoing efforts aim to optimize the benefit-risk profile in other hard-to-treat tumors, in which the 2.0 mg/kg Q3W dosing regimen has demonstrated moderate antitumor activity. OAEs have been observed in patients treated with TV [5] and are a key consideration in the ongoing dose optimization efforts to improve efficacy without significantly increasing risk to patient safety.

Ongoing dose evaluation of alternate regimens in the innovaTV 207 study demonstrated encouraging antitumor activity with a 1.7 mg/kg Q2W TV dosing regimen, with results demonstrating a confirmed objective response rate of



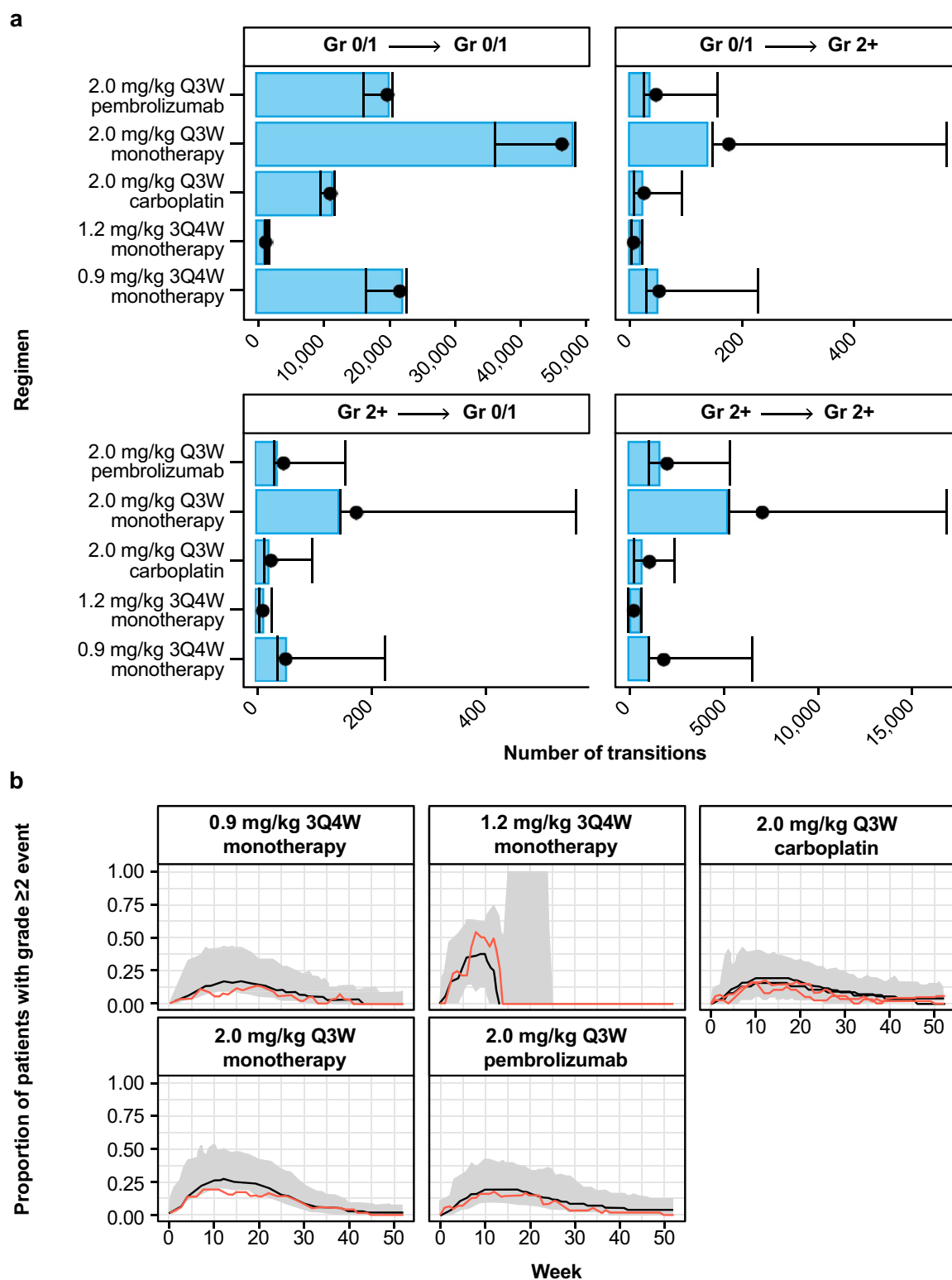


**Fig. 4** OAE final model evaluation: (a) VPC of transition counts by regimens; (b) VPC of longitudinal rate of grade  $\geq 2$  events in monotherapy and combination regimens. (a) Box width indicates the observed frequency of transitions and points. Bars represent the predicted mean and 95% PI. VPCs were calculated conditional on observed covariates, dosing, and censoring times. (b) The red lines indicate observed

probability. The black lines and shaded gray regions indicate the simulated mean and 95% PI. VPCs were calculated conditional on observed covariates, dosing, and censoring times. VPCs for dosing regimens with less than 20 patients were not presented. 3Q4W, days 1, 8, and 15 of a 28-day cycle; Gr, grade; Q3W, every 3 weeks; VPC, visual predictive check

**Fig. 5** Time-to-event of first grade  $\geq 2$  OAE. Time course data are plotted by treatment week. 3Q4W, days 1, 8, and 15 of a 28-day cycle; mono, monotherapy; OAE, ocular adverse event; pembro, pembrolizumab; PI, prediction interval; Q3W, every 3 weeks; TV, tisotumab vedotin

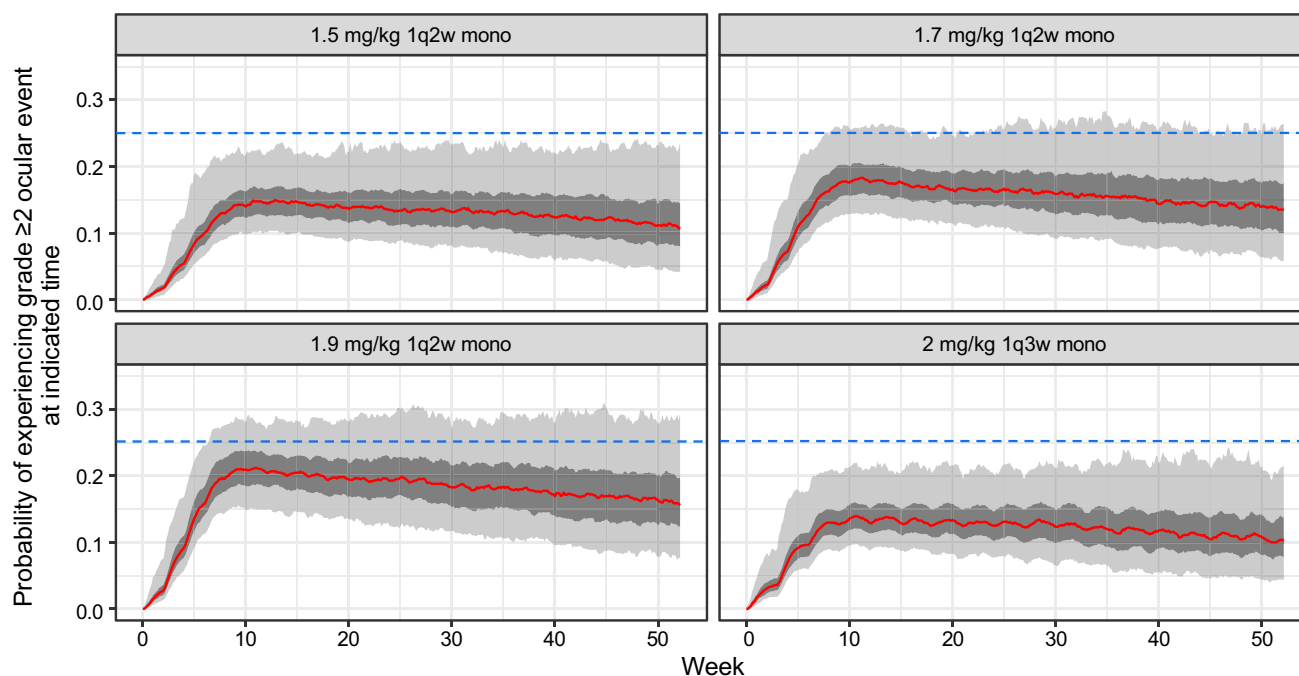
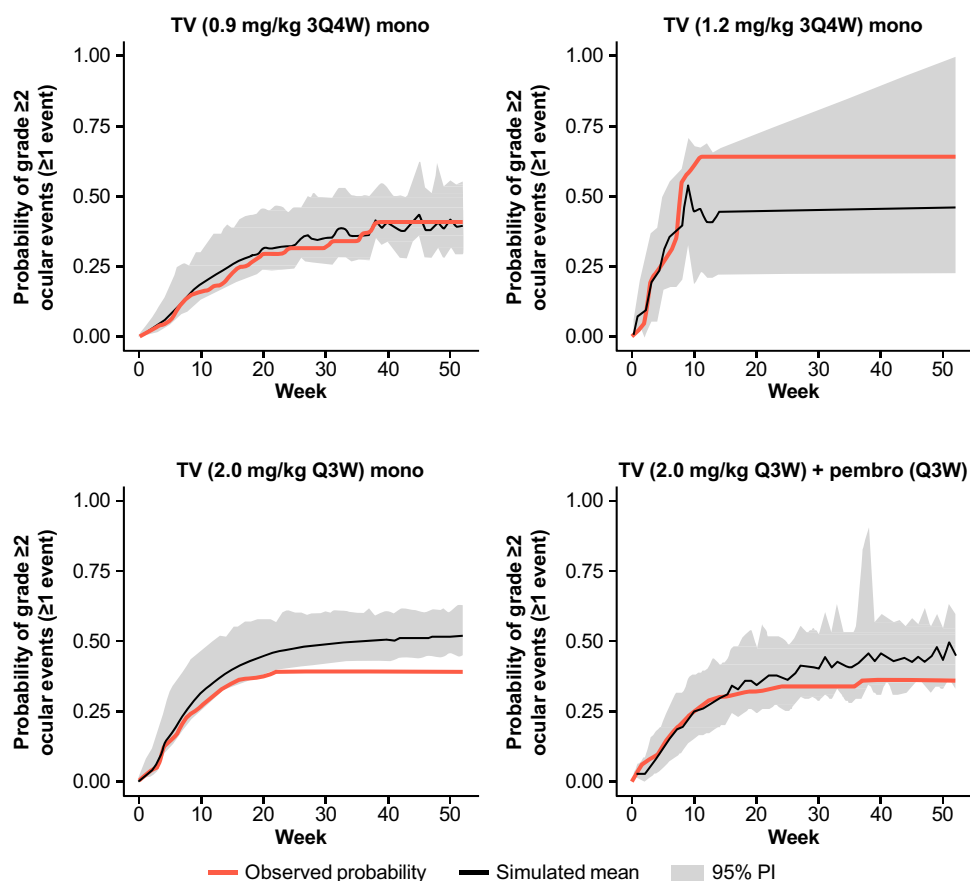


**Fig. 6** Combined simulations: predicted OAE in noncervical cancers. The solid red line and shaded regions represent the median predicted probability of OAE of Grade  $\geq 2$  with 50% and 90% prediction intervals. The dashed blue line, which corresponds to a probability of a Grade  $\geq 2$  OAE of 0.25, is added as a reference line to facilitate visu-

alization of the comparison of predicted OAE profiles at alternative dosing regimens. 1q2w, every 2 weeks; 1q3w, every 3 weeks; mono, monotherapy; OAE, ocular adverse event; pembro, pembrolizumab; PI, prediction interval; Q3W, every 3 weeks; TV, tisotumab vedotin

40% in patients with previously treated recurrent or metastatic head and neck squamous cell carcinoma (second- and third-line subgroups), while maintaining a manageable safety profile [19]. In a previous E-R safety logistic regression analysis, ADC cycle 1 exposures (area under the curve or maximum concentration) were associated with multiple safety endpoints, including probability of grade  $\geq 2$  OAEs, TRAEs leading to dose reduction, and TRAEs leading to dose discontinuation [15]. Additionally, a 1.7 mg/kg Q2W TV dosing regimen was predicted to result in more time above the predicted  $EC_{50}$  and a greater reduction in tumor size, potentially improving efficacy compared with the 2.0 mg/kg Q3W dose in a previous E-R tumor model [18]. To further support TV dose optimization on both dose level and dosing frequency from a safety perspective, rather than assessing E-R relationship with AEs derived from a single time point, the objective of the current modeling work was to characterize the time-course of AE data and evaluate the relationship between exposure and a selected AE endpoint (OAEs).

The present analyses described the longitudinal time course of grade  $\geq 2$  OAEs in TV clinical trials, as well as the time-course of dose reductions and treatment discontinuation due to AEs or disease progression. The established models were then applied to simulate the occurrence of OAEs over time with alternative dosing regimens (Q2W) in noncervical cancer and compare the result with observations with the approved regimen of 2.0 mg/kg Q3W. As shown in the observed OAE profile, the maximal percentage of patients experiencing grade  $\geq 2$  OAEs was reached at approximately 8 weeks after treatment started (Supplementary Fig. 2A), and the final Markov OAE model provided a reasonable description of the observed data across different dosing regimens in both time profile and total number of transitions (Fig. 4). Consistent with previous modeling results, the risk of OAEs increased with exposure to ADC. The daily probability of transitioning into a grade  $\geq 2$  state with no exposure was low (0.0002), but once a patient was in a grade  $\geq 2$  OAE state, the probability of remaining in that state (as opposed to resolving to grade 0 or 1 on the following day) was high, estimated at 0.963 (Table 2). Exposure increased the probability of transition through a time-delayed sigmoidal relationship. A nonproportionality adjustment of the exposure effect (by a factor of 0.215) once in the grade  $\geq 2$  state improved the characterization of the response, improving the model fitting (58 points reduction in AIC, Model 40,071 vs 40,073, Supplementary Table 3) and through a more accurate representation of the of hazard across different OAEs states.

Among all evaluated covariates, only the ECP had a significant effect on reducing the relative risk of OAEs. When TV was combined with pembrolizumab for which OAEs

have been reported [33], a numerically higher but nonsignificant increase to the ADC exposure effect on OAEs, relative to TV monotherapy, was seen (1.07; 90% CI, 0.921–1.22) (Fig. 3). While anti-programmed death-1 or programmed death-ligand 1 treatments are associated with an OAE frequency of approximately 3%, the combination of TV and pembrolizumab did not seem to significantly increase risk of OAEs in patients [34]. Although a majority of patients in this dataset had cervical cancer, tumor location was investigated in the OAE model and was found to be nonsignificant. Patients with cervical cancer were, however, observed to be at higher risk of dose reduction and lower hazard of discontinuation due to AE in this dataset (Supplementary Table 5 and Fig. 6). Interpretation of this result may be limited by differences in treatment duration of different tumor types and sample size at various dose levels. Predicting OAEs using the current modeling framework allowed presentation of the longitudinal risk of OAEs with alternative dosing regimens while accounting for multiple components that may impact the risk of OAEs, including effect of ADC exposure and indirect effects of ADC exposure from dose reduction or discontinuation.

Some limitations were noted in this analysis. Among the seven clinical studies included in the analysis, none were specifically designed or powered to detect differences in grade  $\geq 2$  OAEs between dosing regimens. As such, it was not feasible to apply rigorous statistical criteria or formal hypothesis testing within the scope of this analysis; this analysis is instead exploratory in nature.

Additionally, exposures used in modeling were collected in a setting in which protocol-specified dose reductions due to safety events have occurred. While OAEs are one mechanism that can cause dose reductions, there are others as well: exploratory analyses suggested that at most, half of the dose reductions occur due to OAEs (Table S5). This analysis assumed a causal effect of dose on exposure and a causal effect of exposure on OAEs. The effect of OAEs on dose reductions were not directly modeled, with the effect presumably pre-specified to a large extent in the study protocol. However, due to the multiple mediators of the exposure effect on dose reductions and our aim of describing OAE occurrence as a result of dose and dose reduction strategy, the pooled effect of the dose reduction strategy was modeled using an exposure-dose reduction model. Although this is a more practical (albeit more assumption-heavy) alternative to modeling the entirety of all individual exposure-safety-dose reduction submodels, the accuracy of predictions for new regimens did rely upon the validity of the assumed safety-dose relationship in doses yet to be studied.

Furthermore, the implementation of the ECP was modeled as a covariate effect on the overall hazard or odds of

event, which is a simplification of its impact on the risk of OAEs. When simulating patient outcomes, dose delays and interruptions as well as maximum dose holding period allowed per study protocols were not accounted for. Indeed, considering the dose-reduction process as multi-state (i.e., no reductions, holding dose, first reduction, second reduction) could have better reflected the actual ECP practice but only with substantial additional model development. Another apparent bias was the overprediction of the total number of patients who would have at least one grade  $\geq 2$  OAE, an effect that was apparent in the time-to-first OAE VPCs with the 2.0 mg/kg Q3W monotherapy regimen. Although the number of patients who had a grade  $\geq 2$  OAE at any point in the study was not presented as an output from the combined simulations, and the overall incidence across patients remaining under observation appeared to have been accurately modeled, predictions of the number of patients who would (at some point) have a grade  $\geq 2$  OAE may have been artificially high and should be interpreted conservatively. The overprediction noted here is possibly a result of the censoring mechanism in the predictive checks. As the predictive checks were performed conditional on observed censoring, virtual patients may remain under observation longer than they would in actual trial scenarios, increasing the likelihood of observing an OAE. Another limitation in this analysis was that, across studies, end dates of OAEs were missing in approximately 20–30% of the recorded events. These were assumed to be missing at random within the studies and were imputed at the study median durations. A more complex missing mechanism (i.e., missing not at random) may imply bias in the predicted durations of events. For the purposes of this analysis, however, the identification of the concentration-driven onset and frequency of OAEs was of principal concern. The direct and indirect effects of MMAE exposure were also assessed, and as observed in the previous E-R analysis [16], the risk of OAEs decreased with exposure to MMAE. This counterintuitive relationship between MMAE and other AEs has been observed with other vedotins [35]. Further evaluation of the relationship between OAEs and MMAE could be challenging as the mechanism(s) of OAEs are not fully understood.

## Conclusions

This Markov model explored the occurrence, severity, and duration of OAEs across seven TV clinical studies and supports the use of an alternative to existing E-R approaches to assessing the risk of OAEs with exposure to ADC and MMAE. Of the multiple covariates modeled, results indicated that implementation of the ECP significantly reduced

the risk of grade  $\geq 2$  OAEs, whereas other covariates did not lead to a statistically significant reduction of risk. The alternate TV dosing regimen of 1.7 mg/kg Q2W explored in the current analysis is being evaluated clinically in the ongoing innovaTV 207 clinical trial to further establish how this impacts the benefit:risk profile.

**Supplementary Information** The online version contains supplementary material available at <https://doi.org/10.1007/s10928-025-10003-w>.

**Acknowledgements** This study was sponsored by Seagen Inc. (acquired by Pfizer in December 2023) and Genmab, the codevelopers of tisotumab vedotin. The authors would like to thank all patients who participated in the TV clinical studies and their families. The authors also thank Leonardo Nicacio for review of the manuscript. Medical writing assistance funded by Pfizer according to Good Publication Practice guidelines was provided by Uzezi Cedras, MSc, Martina Kusi-Mensah, PharmD, Melissa Ward, BA (all of Scion, London, UK) and Blaise Low, PhD (Nucleus Global, an Inizio Company). The sponsor was involved in the study design and collection, analysis, and interpretation of data, as well as data checking of information provided in the manuscript. However, ultimate responsibility for opinions, conclusions, and data interpretation lies with the authors.

**Author contributions** RG, JV, DP, SF, CP, MG, and IS conceptualized the study, RG, DP, SF, and CO developed the study methodology, DP contributed to the study investigation, project administration, software programming, and validated, analyzed, curated, and visualized the data, DP and AG provided the study resources, RG, JV, WDH, SF, CP, and A-SC supervised the study, DP, SF, and RG drafted the manuscript, and all authors reviewed and edited the manuscript.

**Funding** This study was funded by Genmab (Copenhagen, Denmark) and Pfizer Inc.

**Data and/or code availability** Metrum Research Group performed validation of the code and data related to these analyses, and both are stored in version-controlled repositories on redundant storage. Upon request and subject to review, Pfizer will provide the data that support the findings of this study. Subject to certain criteria, conditions, and exceptions, Pfizer may also provide access to the related individual de-identified participant data. See <https://www.pfizer.com/science/clinical-trials/trial-data-and-results> for more information.

## Declarations

**Ethics approval** All clinical studies were conducted in accordance with good clinical practice guidelines from the International Council for Harmonization of Technical Requirements for Pharmaceuticals for Human Use and the principles of the Declaration of Helsinki. Protocols were approved by relevant regulatory and independent ethics committees.

**Competing interests** SF, AG, IS, and MG report employment and stocks or stock options with Genmab US Inc. RG, JV, CO, and A-SC report employment and stocks or stock options with Pfizer Inc. CP reports employment and stocks or stock options with Genmab US Inc. and grants, consulting fees, and honoraria from Metrum LLC. DP reports employment with Metrum Research Group. WDH reports employment with BeiGene and former employment and stock options with Seagen at the time of study.

**Open Access** This article is licensed under a Creative Commons Attribution-NonCommercial-NoDerivatives 4.0 International License, which permits any non-commercial use, sharing, distribution and reproduction in any medium or format, as long as you give appropriate credit to the original author(s) and the source, provide a link to the Creative Commons licence, and indicate if you modified the licensed material. You do not have permission under this licence to share adapted material derived from this article or parts of it. The images or other third party material in this article are included in the article's Creative Commons licence, unless indicated otherwise in a credit line to the material. If material is not included in the article's Creative Commons licence and your intended use is not permitted by statutory regulation or exceeds the permitted use, you will need to obtain permission directly from the copyright holder. To view a copy of this licence, visit <http://creativecommons.org/licenses/by-nc-nd/4.0/>.

## References

1. Breij EC, de Goeij BE, Verploegen S, Schuurhuis DH, Amirkhosravi A, Francis J, Miller VB, Houtkamp M, Bleeker WK, Satijn D, Parren PW (2014) An antibody-drug conjugate that targets tissue factor exhibits potent therapeutic activity against a broad range of solid tumors. *Cancer Res* 74(4):1214–1226. <https://doi.org/10.1158/0008-5472.CAN-13-2440>
2. de Goeij BE, Satijn D, Freitag CM, Wubbolts R, Bleeker WK, Khasanov A, Zhu T, Chen G, Miao D, van Berkel PH, Parren PW (2015) High turnover of tissue factor enables efficient intracellular delivery of antibody-drug conjugates. *Mol Cancer Ther* 14(5):1130–1140. <https://doi.org/10.1158/1535-7163.MCT-14-0798>
3. Alley SC, Harris JR, Cao A, van den Heuvel EG, Velayudhan J, Satijn D, Verploegen S, Dominguez T, Breij EC (2019) Abstract 221: tisotumab vedotin induces anti-tumor activity through MMAE-mediated, Fc-mediated, and Fab-mediated effector functions *in vitro*. *Cancer Res* 79(suppl 13):221–221. <https://doi.org/10.1158/1538-7445.AM2019-221>
4. Seagen Inc (2024) TIVDAK (tisotumab vedotin). Prescribing information. <https://labeling.pfizer.com/ShowLabeling.aspx?id=20632>. Accessed 26 July 2024
5. Coleman RL, Lorusso D, Gennigens C, Gonzalez-Martin A, Randall L, Cibula D, Lund B, Woelber L, Pignata S, Forget F, Redondo A, Vindelov SD, Chen M, Harris JR, Smith M, Nicacio LV, Teng MSL, Laenen A, Rangwala R, Manso L, Mirza M, Monk BJ, Vergote I, innovaTV 204/GOG-3023/ENGOT-cx6 Collaborators (2021) Efficacy and safety of tisotumab vedotin in previously treated recurrent or metastatic cervical cancer (innovaTV 204/GOG-3023/ENGOT-cx6): a multicentre, open-label, single-arm, phase 2 study. *Lancet Oncol* 22(5):609–619. [https://doi.org/10.1016/S1470-2045\(21\)00056-5](https://doi.org/10.1016/S1470-2045(21)00056-5)
6. ClinicalTrials.gov (2018) Efficacy and safety study of tisotumab vedotin for patients with solid tumors (innovaTV 207). <https://www.clinicaltrials.gov/ct2/show/NCT03485209>. Accessed 12 May 2024
7. Dominguez-Llamas S, Caro-Magdaleno M, Mataix-Albert B, Aviles-Prieto J, Romero-Barranca I, Rodriguez-de-la-Rua E (2023) Adverse events of antibody-drug conjugates on the ocular surface in cancer therapy. *Clin Transl Oncol* 25(11):3086–3100. <https://doi.org/10.1007/s12094-023-03261-y>
8. Eaton JS, Miller PE, Mannis MJ, Murphy CJ (2015) Ocular adverse events associated with antibody-drug conjugates in human clinical trials. *J Ocul Pharmacol Ther* 31(10):589–604. <https://doi.org/10.1089/jop.2015.0064>
9. Förster Y, Meyer A, Albrecht S, Schwenzer B (2006) Tissue factor and tumor: clinical and laboratory aspects. *Clin Chim Acta* 364(1–2):12–21. <https://doi.org/10.1016/j.cca.2005.05.018>
10. Patry G, Hovington H, Larue H, Harel F, Fradet Y, Lacombe L (2008) Tissue factor expression correlates with disease-specific survival in patients with node-negative muscle-invasive bladder cancer. *Int J Cancer* 122(7):1592–1597. <https://doi.org/10.1002/ijc.23240>
11. van den Berg YW, Osanto S, Reitsma PH, Versteeg HH (2012) The relationship between tissue factor and cancer progression: insights from bench and bedside. *Blood* 119(4):924–932. <https://doi.org/10.1182/blood-2011-06-317685>
12. Lwaleed BA, Cooper AJ, Voegeli D, Getliffe K (2007) Tissue factor: a critical role in inflammation and cancer. *Biol Res Nurs* 9(2):97–107. <https://doi.org/10.1177/1099800407305733>
13. Butenas S (2012) Tissue factor structure and function. *Scientifica* 2012:964862. <https://doi.org/10.6064/2012/964862>
14. Hong DS, Concini N, Vergote I, de Bono JS, Slomovitz BM, Drew Y, Arkenau HT, Machiels JP, Spicer JF, Jones R, Forster MD, Cornez N, Gennigens C, Johnson ML, Thistlethwaite FC, Rangwala RA, Ghatta S, Windfeld K, Harris JR, Lassen UN, Coleman RL (2020) Tisotumab vedotin in previously treated recurrent or metastatic cervical cancer. *Clin Cancer Res* 26(6):1220–1228. <https://doi.org/10.1158/1078-0432.CCR-19-2962>
15. Vergote I, González-Martín A, Fujiwara K, Kalbacher E, Bagaméri A, Ghamande S, Lee J-Y, Banerjee S, Maluf FC, Lorusso D, Yonemori K, Nieuwenhuysen EV, Manso L, Woelber L, Westermann A, Covens A, Hasegawa K, Kim B-G, Raimondo M, Bjurberg M, Cruz FM, Angelergues A, Cibula D, Barraclough L, Oaknin A, Gennigens C, Nicacio L, Teng MSL, Whalley E, Soumaoro I, Slomovitz BM (2024) Tisotumab vedotin as second- or third-line therapy for recurrent cervical cancer. *N Engl J Med* 391(1):44–55. <https://doi.org/10.1056/NEJMoa2313811>
16. Passey C, Voellinger J, Gibiansky L, Gunawan R, Nicacio L, Soumaoro I, Hanley WD, Winter H, Gupta M (2023) Exposure-safety and exposure-efficacy analyses for tisotumab vedotin for patients with locally advanced or metastatic solid tumors. *CPT Pharmacometrics Syst Pharmacol* 12(9):1262–1273. <https://doi.org/10.1002/psp4.13007>
17. Hong DS, Birnbaum A, Steuer C, Taylor M, George TJ, Lacy J, Wang B, Beca F, Nicacio L, Soumaoro I, Cho M (2022) Efficacy and safety of tisotumab vedotin in patients with head and neck squamous cell carcinoma: results from a phase II cohort. *Int J Radiat Oncol Biol Phys* 112(5):e10–e11. <https://doi.org/10.1016/j.ijrobp.2021.12.028>
18. Voellinger J, Passey C, Feng YS, Gunawan R, Gibiansky L, Polhamus D, Gerritsen A, O'Day C, Nicacio L, Soumaoro I, Gupta M, Hanley W (2023) 5P tisotumab vedotin (TV) dose schedule optimization in non-cervical populations. *ESMO Open* 8(1):100971. <https://doi.org/10.1016/j.esmoop.2023.100971>
19. Sun L, Fayette J, Salas S, Hong DS, Adkins D, Dunn L, Ciardiello F, Cirauqui B, William WNJ, Saba NF, Chung CH, Birnbaum AE, Zandberg DP, Wehr A, Nicacio LV, Soumaoro I, Carret A-S, Seiwert TY (2024) Tisotumab vedotin in head and neck squamous cell carcinoma: updated analysis from innovaTV 207 part C. *J Clin Oncol* 42(suppl 16):6012. [https://doi.org/10.1200/JCO.2024.42.16\\_suppl.6012](https://doi.org/10.1200/JCO.2024.42.16_suppl.6012)
20. ClinicalTrials.gov (2015) Tisotumab vedotin (HuMax®-TF-ADC) safety study in patients with solid tumors (innovaTV 202). <https://clinicaltrials.gov/study/NCT02552121>. Accessed 7 August 2024
21. ClinicalTrials.gov (2018) Safety and efficacy of tisotumab vedotin monotherapy & in combination with other cancer agents in subjects with cervical cancer (innovaTV 205). <https://clinicaltrials.gov/study/NCT03786081>. Accessed 7 August 2024
22. ClinicalTrials.gov (2019) A trial of tisotumab vedotin in Japanese subjects with advanced solid malignancies (innovaTV 206). <https://clinicaltrials.gov/study/NCT03913741>. Accessed 7 August 2024
23. ClinicalTrials.gov (2018) A study of weekly tisotumab vedotin for patients with platinum-resistant ovarian cancer with safety



- run-in (innovaTV 208). <https://clinicaltrials.gov/study/NCT03657043>. Accessed 7 August 2024
24. Gibiansky L, Passey C, Voellinger J, Gunawan R, Hanley WD, Gupta M, Winter H (2022) Population pharmacokinetic analysis for tisotumab vedotin in patients with locally advanced and/or metastatic solid tumors. *CPT Pharmacometrics Syst Pharmacol* 11(10):1358–1370. <https://doi.org/10.1002/psp4.12850>
  25. Lu T, Yang Y, Jin JY, Kagedal M (2020) Analysis of longitudinal-ordered categorical data for muscle spasm adverse event of vismodegib: comparison between different pharmacometric models. *CPT Pharmacometrics Syst Pharmacol* 9(2):96–105. <https://doi.org/10.1002/psp4.12487>
  26. Karlsson MO, Schoemaker RC, Kemp B, Cohen AF, van Gerven JM, Tuk B, Peck CC, Danhof M (2000) A pharmacodynamic Markov mixed-effects model for the effect of temazepam on sleep. *Clin Pharmacol Ther* 68(2):175–188. <https://doi.org/10.1067/mcp.2000.108669>
  27. Gastonguay MR (2004) A full model estimation approach for covariate effects: inference based on clinical importance and estimation precision. *AAPS* 6(S1):W4354. [https://www.metrumrg.com/wp-content/uploads/2018/08/aaps\\_2004\\_fullmodel.pdf](https://www.metrumrg.com/wp-content/uploads/2018/08/aaps_2004_fullmodel.pdf)
  28. Peterson B, Harrell FE Jr. (1990) Partial proportional odds models for ordinal response variables. *J Roy Stat Soc: Ser C (Appl Stat)* 39(2):205–217. <https://doi.org/10.2307/2347760>
  29. Savic RM, Jonker DM, Kerbusch T, Karlsson MO (2007) Implementation of a transit compartment model for describing drug absorption in pharmacokinetic studies. *J Pharmacokinet Pharmacodyn* 34(5):711–726. <https://doi.org/10.1007/s10928-007-9066-0>
  30. Baron K, Gastonguay M (2015) Simulation from ODE-based population PK/PD and systems pharmacology models in R with mrgsolve. *J Pharmacokinet Pharmacodyn* 42:S84–S85
  31. Korn EL, Moscow JA, Freidlin B (2023) Dose optimization during drug development: whether and when to optimize. *J Natl Cancer Inst* 115(5):492–497. <https://doi.org/10.1093/jnci/djac232>
  32. Aggarwal D, Yang J, Salam MA, Sengupta S, Al-Amin MY, Mustafa S, Khan MA, Huang X, Pawar JS (2023) Antibody-drug conjugates: the paradigm shifts in the targeted cancer therapy. *Front Immunol* 14:1203073. <https://doi.org/10.3389/fimmu.2023.1203073>
  33. KEYTRUDA® (pembrolizumab) [prescribing information] (2024) Rahway, NJ: Merck Sharp & Dohme LLC. [https://www.accessdata.fda.gov/drugsatfda\\_docs/label/2025/125514s1721bl.pdf](https://www.accessdata.fda.gov/drugsatfda_docs/label/2025/125514s1721bl.pdf)
  34. Young L, Finnigan S, Streicher H, Chen HX, Murray J, Sen HN, Sharon E (2021) Ocular adverse events in PD-1 and PD-L1 inhibitors. *J Immunother Cancer* 9(7):e002119. <https://doi.org/10.1136/jitc-2020-002119>
  35. Suri A, Mould DR, Liu Y, Jang G, Venkatakrishnan K (2018) Population PK and exposure-response relationships for the antibody-drug conjugate brentuximab vedotin in CTCL patients in the phase III ALCANZA study. *Clin Pharmacol Ther* 104(5):989–999. <https://doi.org/10.1002/cpt.1037>
  36. ClinicalTrials.gov (2018) A trial of tisotumab vedotin in cervical cancer (innovaTV 204). <https://clinicaltrials.gov/study/NCT03438396>. Accessed 7 August 2024

**Publisher's Note** Springer Nature remains neutral with regard to jurisdictional claims in published maps and institutional affiliations.